View Article Online / Journal Homepage / Table of Contents for this issue
Dynamic Article Links

Analyst

Cite this: *Analyst*, 2012, **137**, 1837

www.rsc.org/analyst

PAPER

Published on 08 February 2012. Downloaded by State University of New York at Stony Brook on 30/10/2014 15:40:16.

Two-photon fluorescent probe for cadmium imaging in cells

Yongyou Liu,[a] Xiaohu Dong,[a] Jian Sun,[b] Cheng Zhong,[c] Boheng Li,[a] Ximeng You,[a] Bifeng Liu[b] and Zhihong Liu*[a]

Received 15th December 2011, Accepted 4th February 2012
DOI: 10.1039/c2an16254g

A novel two-photon excited fluorescent probe for cadmium (named as **TPCd**) was designed and synthesized utilizing a prodan (6-acetyl-2-methoxynaphthalene) derivative as the two-photon fluorophore and an *o*-phenylenediamine derivative as the Cd^{2+} chelator, which possessed favorable photophysical properties and good water-solubility. The probe was designed with a photoinduced electron transfer (PET) mechanism and thus was weakly fluorescent itself. After binding with Cd^{2+} which blocked the PET process, the fluorescence intensity of the probe was enhanced by up to 15-fold under one-photon excitation (OPE) and 27-fold under two-photon excitation (TPE), respectively. The two-photon action cross-section ($\Phi\delta$) of the **TPCd**–Cd complex at 740 nm reached 109 GM compared to 3.6 GM for free **TPCd**, indicating the promising prospect of the probe in two-photon application. **TPCd** chelated Cd^{2+} with 1 : 1 stoichiometry, and the apparent dissociation constant (K_d) was 6.1×10^{-5} M for the one-photon mode and 7.2×10^{-5} M for the two-photon mode. The probe responded to Cd^{2+} over a wide linear range from 0.1 to 30 μM with a detection limit of 0.04 μM. High selectivity of the probe towards Cd^{2+} was acquired in Tris-HCl/sodium phosphate buffer. The probe was pH-independent in the biologically relevant pH range and non-toxic to living cells at reasonable concentration levels, warranting its *in vivo* applications. Through two-photon microscopy imaging, the probe was successfully applied to detect Cd^{2+} uptake in living HepG2 cells.

Introduction

Cadmium has been recognized as a highly toxic heavy metal whose half-life in the human body is estimated to be 15–30 years.[1] Excessive exposure to cadmium will lead to pulmonary cancer and probably cause some non-pulmonary cancers, such as prostatic and renal cancers, owing to the increased Cd^{2+} accumulation within the human body.[2] Nowadays, cadmium is widely used in industry and agriculture, and the resulting high level of cadmium contamination in soil and crops has raised great concern. However, the mechanisms involved in Cd^{2+}-uptake and carcinogenesis remain undefined. Therefore, developing reliable methods for Cd^{2+} quantification in environmental samples and in cells/tissues is of great significance for clarifying Cd^{2+} carcinogenesis and other biological effects. Several methods such as atomic absorption[3] and ICP (inductively coupled plasma) atomic emission spectroscopy[4] have been used to detect cadmium, possessing good sensitivity and giving accurate results. However, these methods need rather stringent sample pretreatment, which prevents them from being utilized in real-time and *in vivo* applications. In the past decades, fluorescent sensing *via* suitable sensors and probes has attracted increasing interest for the detection of various targets due to its simple operation and high sensitivity and specificity. More importantly, as a kind of non-destructive and visualizable technique, fluorescence is considered to be most suitable for real-time detection in cells or tissues.[5]

The use of fluorescent Cd^{2+} probes would help to reveal the cadmium carcinogen mechanism *in vivo* as well as to monitor cadmium concentration temporally in the environment. Moreover, it could be an ideal tool for evaluating and dynamically mapping the intracellular fluctuations of the metal ion by using microscopy. So far, a few fluorescent Cd^{2+} probes have been reported utilizing several fluorophores and recognition ligands. A BODIPY-based sensor was developed which responded to Cd^{2+} showing an evident fluorescence enhancement according to a photoinduced electron transfer mechanism.[6] Naphthalimide was used as the emitter of another Cd^{2+} probe, which exhibited favorable photophysical properties with a sensitive response to Cd^{2+} and could effectively discriminate Cd^{2+} from Zn^{2+}.[7] Di-2-picolylamine (DPA) derivatives were employed as the chelators of some Cd^{2+} probes designed with the internal charge transfer

[a]*Key Laboratory of Analytical Chemistry for Biology and Medicine (Ministry of Education), College of Chemistry and Molecular Sciences, Wuhan University, Wuhan, 430072, P. R. China. E-mail: zhhliu@whu.edu.cn; Fax: +86-27-68754067; Tel: +86-27-87217886*
[b]*The Key Laboratory of Biomedical Photonics of MOE – Hubei Bioinformatics & Molecular Imaging Key Laboratory – Division of Biomedical Photonics at Wuhan National Laboratory for Optoelectronics, Department of Systems Biology, College of Life Science & Technology, Huazhong University of Science & Technology, Wuhan, 430074, China*
[c]*Hubei Key Lab of Organic and Polymeric Optoelectronic Materials, Wuhan University, Wuhan, 430072, P. R. China*

View Article Online

Published on 08 February 2012. Downloaded by State University of New York at Stony Brook on 30/10/2014 15:40:16.

(ICT) principle, which displayed a notable spectral shift either in absorption[8] or in emission[9] spectra and therefore could ratiometrically detect Cd^{2+}. Another fine Cd^{2+} sensor was constructed on the basis of a monomer–excimer switch system. When Cd^{2+} interacts with a calixarene receptor, the excimer formed by an excited and a ground state pyrene is separated to monomer unit, resulting in a remarkable signal change.[10]

For most of these probes, however, their practical application is still limited, more or less due to their poor water solubility or pH-dependent fluorescence in physiological environments. As a result, only very few of them have been used for *in vivo* imaging.[6] And what is more important, all these reported fluorescent probes require excitation with short-wavelength UV/Vis light (that is, *ca.* 350–500 nm). As has been widely recognized, the utilization of UV/Vis excitation with one-photon excitation mode may cause several concerns when the probes are applied in living cells or tissues. For example, the high-energy UV light is likely to cause photodamage to biological substances or samples as well as photobleaching of fluorophores, which hinders the prolonged observation of biological events. Another general problem of one-photon excitation (OPE) fluorescence could be the rather serious background fluorescence and scattering light arising from biological samples, which lowers the sensitivity or even disables the detection.[11] To circumvent these problems, two-photon excitation (TPE) fluorescence, which utilizes two lower-energy near-infrared photons for excitation to give emission in the visible region, has received increasing attention. TPE molecules can be excited in the near-infrared (NIR) or infrared region. In this excitation window autofluorescence of biomolecules is avoided and the scattering light is dramatically reduced, which leads to a higher signal-to-noise ratio and improved detection sensitivity. In the past several years, we and other groups have proven the advantages of TPE fluorescence in quantitative bioassays.[12,13]

Besides the above-mentioned photophysical merits of TPE fluorescence, it also features much less photobleaching off the focal plane and less photodamage to biological samples due to the relatively lower energy of the NIR/IR photons. The fact that two-photon absorption occurs only at an extremely small focal volume (femtoliter) endows the TPE technique with higher spatial resolution.[14,15] Further considering the higher penetrating depth of NIR/IR light compared to UV/Vis light (greater than 500 μm), two-photon excited fluorescent probes would be competitive alternatives for cell/tissue imaging. As pioneering works, Cho and co-workers have reported a series of two-photon fluorescent probes for some cations including Ca^{2+}, Mg^{2+}, *etc.*, with favorable properties and successful applications in bioimaging.[16–21] Thereafter, several two-photon fluorescent probes have been reported by other groups.[22–25] Their advantages over one-photon probes, such as increased penetration depth, localized excitation and higher resolution, prolonged observation time, *etc.*, have been well established, suggesting good prospects for TPE probes. To the best of our knowledge, however, there have been no reports on two-photon fluorescent probes for cadmium yet. Herein, we report for the first time a two-photon excited Cd^{2+} fluorescent probe (named as **TPCd**, see Scheme 1 for synthesis details). The probe is designed with a photoinduced electron transfer principle, which functions as a fluorescent off–on switch upon Cd^{2+} binding. In addition, the probe is highly water-soluble, non-toxic to living cells and pH-stable within the physiological pH range. These features make **TPCd** a suitable two-photon fluorescent probe for intracellular Cd^{2+} imaging, which is established through detecting Cd^{2+} uptake in living HepG2 cells.

Experimental

Synthesis of TPCd.

Materials. All the solvents and reagents were of analytic grade and used without further purification unless for special needs. 6-Acetyl-2-methoxynaphthalene was purchased from Alfa Aesar (Ward Hill, MA). Other regents were bought from Sinopharm Chemical Reagent Co. (Shanghai, China).

Synthetic procedures. The synthesis route for **TPCd** is illustrated in Scheme 1.

6-Acetyl-2-hydroxynaphthalene (I)

6-Acetyl-2-methoxynaphthalene (1.00 g, 5 mmol) was dissolved in 4 mL CH_2Cl_2, the mixture was added dropwise into 36% HCl (80 mL, 0.93 mol) under stirring. Then triethylamine (0.75 mL, 5.4 mmol) was added dropwise into the solution. The mixture was stirred at 85 °C for 4 h, and the excess acid was neutralized with solid NaOH. The solution was extracted with ethyl acetate and washed with saturated $NaHCO_3$ and brine. The organic layer was dried with anhydrous Na_2SO_4 and the solvent was removed in vacuum. The crude product was purified by column chromatography using petroleum ether–EtOAc 5 : 1 (v/v) as the eluant to yield compound **I** (839.7 mg, 90.2%). ^1H NMR (300 MHz, $CDCl_3$): δ 8.36 (s, 1H), 7.95 (d, 1H, $J = 8.7$ Hz), 7.84

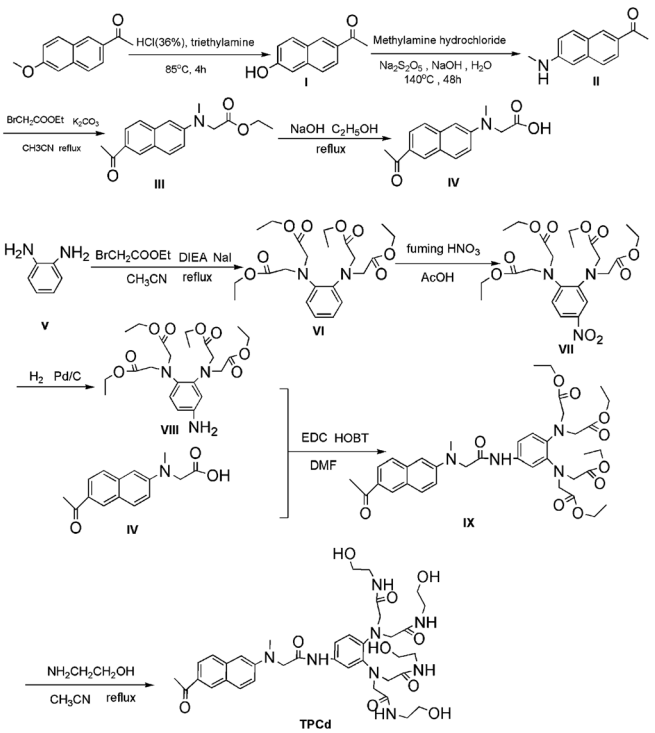

Scheme 1 The synthesis route for **TPCd**.

 This journal is © The Royal Society of Chemistry 2012

View Article Online

Published on 08 February 2012. Downloaded by State University of New York at Stony Brook on 30/10/2014 15:40:16.

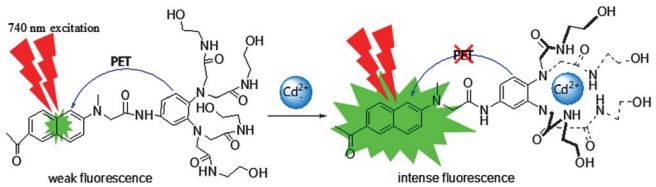

Scheme 2 Illustration of Cd^{2+} sensing principle with **TPCd** probe.

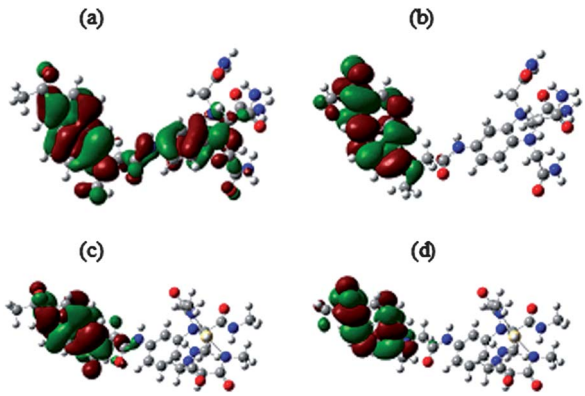

Fig. 1 The geometries and frontier orbitals of **TPCd** and **TPCd**–Cd^{2+}: (a) HOMO of **TPCd**; (b) LUMO of **TPCd**; (c) HOMO of **TPCd**–Cd^{2+}; (d) LUMO of **TPCd**–Cd^{2+}.

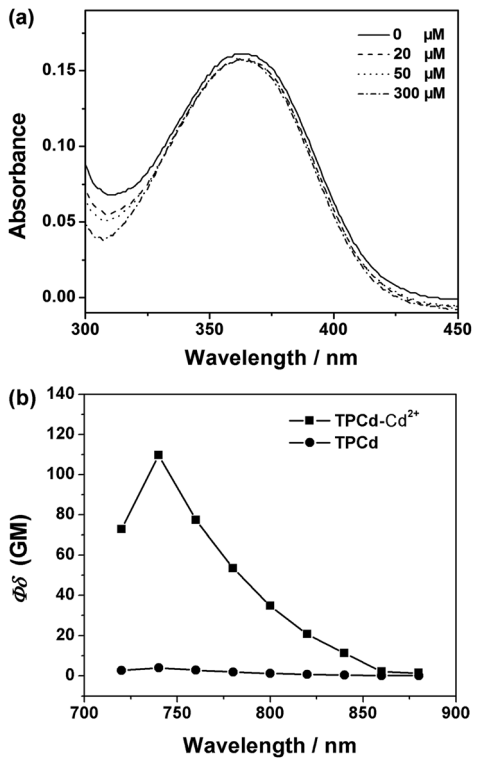

Fig. 2 (a) Absorption spectra of **TPCd** in the presence of varying concentrations of free Cd^{2+}. (b) Two-photon action cross-section of **TPCd** in the absence (●) and presence (■) of Cd^{2+}. These data were measured in Tris-HCl (0.02 M) solution (containing 0.1 mM sodium phosphate, pH = 7.4).

(d, 1H, J = 9.3 Hz), 7.673 (d, 1H, J = 8.4 Hz), 7.15 (s, 1H), 7.14 (d, 1H, J = 6.9 Hz), 5.53 (s, 1H), 2.66 (s, 3H).

6-Acetyl-*N*-methyl-2-naphthylamine (II)

A mixture of compound **I** (839.7 mg, 4.51 mmol), $Na_2S_2O_5$ (1.72 g, 9.05 mmol), NaOH (0.906 g, 22.7 mmol), $MeNH_2 \cdot HCl$ (1.37 g, 20.3mmol) and H_2O (30 mL) was added into a hydrothermal autoclave and stirred at 140 °C for 48 h. The solid product was collected by filtration and washed with water till the filtrate was neutral. Then the crude product was purified by column chromatography using petroleum ether–EtOAc 8 : 1 (v/v) as the eluant to yield compound **II** (570 mg, 63.5%). ^{1}H NMR (300 MHz, $CDCl_3$): δ 8.307 (s, 1H), 7.93 (d, 1H, J = 8.1 Hz), 7.72 (d, 1H, J = 8.4 Hz), 7.64 (d, 1H, J = 8.7 Hz), 6.912 (d, 1H, J = 9.0 Hz), 6.77 (s, 1H), 4.17 (s, 1H), 2.972 (s, 3H), 2.67 (s, 3H).

6-Acetyl-2-[*N*-methyl-*N*-(carboxy)amino]naphthalene (III)

A mixture of **II** (2 g, 10 mmol), ethyl bromoacetate (3.4 g, 20 mmol), K_2CO_3 (2.8 g, 20 mmol), NaI (0.6 g, 4 mmol) in MeCN (60 mL) was refluxed under Ar atmosphere for 18 h. The product was extracted with ethyl acetate and washed with brine. After drying and evaporation, the residue was chromatographed on silica in petroleum ether–EtOAc 4 : 1 (v/v) to yield 2.8 g **III**, 73%. ^{1}H NMR (300 MHz, $CDCl_3$): δ 8.32 (d, 1H, J = 2 Hz),7.92 (dd, 1H, J = 9 Hz, J = 2 Hz), 7.80 (d, 1H, J = 9 Hz), 7.64 (d, 1H, J = 9 Hz), 7.08 (dd, 1H, J = 9 Hz, J = 2 Hz), 6.88 (d, 1H, J = 2 Hz), 4.23 (m, 4H), 3.74 (s, 3H), 3.21 (s, 3H), 2.67 (s, 3H), 1.23 (t, 3H). MS (ESI+) Calcd for $C_{17}H_{19}NO_3$ ($[M + H]^+$, 286.1; Found: 286.1.

6-Acetyl-2-[*N*-methyl-*N*-(carboxymethyl)amino]naphthalene (IV)

A mixture of **III** (1g, 3.5 mmol) and KOH (0.4 g, 7 mmol) in EtOH/H_2O (15 : 3 mL) was stirred for 5 h. The resultant solution was diluted with ice-water (50 mL) and concentrated HCl (aq.) was added slowly at 0 °C until pH = 3. The precipitate was collected, washed with distilled water and purified by crystallization from MeOH to yield **IV** (0.9 g, 80%). ^{1}H NMR (300 MHz, DMSO-d_6): δ 8.45(s, 1H), 7.9 (d, 1H, J = 9 Hz), 7.81 (d, 1H, J = 9 Hz), 7.67 (d, 1H, J = 9 Hz), 7.21 (d, 1H, J = 9 Hz), 6.96 (s, 1H), 4.29 (s, 2H), 3.12 (s, 3H), 2.62 (s, 3H); MS (ESI−) Calcd for $C_{15}H_{15}NO_3$ ($[M - H]^+$, 256.2; Found: 256.2.

N,*N*,*N*′,*N*′-Tetra{(2-hydroxyethyl)carbamoylmethyl}-*o*-phenylenediamine (VI)

A solution of **V** (2g, 18.5 mmol), ethyl bromoacetate (13.4 mL, 120 mmol) sodium iodide (2.5 g, 17 mmol) and diisopropylethylamine (17 ml, 100 mmol) in 20 mL acetonitrile was refluxed under nitrogen for 7 h, then cooled and poured into 100 mL water. The resulting mixture was extracted with dichloromethane (3 × 50 mL). The extract was dried over sodium sulfate and was concentrated to give brown oil, which was purified by column chromatography using petroleum ether–EtOAc 5 : 1 (v/v) as eluant. **VI** (8.3 g, 85%) was yielded as a white solid. ^{1}H NMR (300 MHz $CDCl_3$): δ 7.03–7.06 (m, 2 H), 6.93–6.96 (m, 2 H), 4.30 (s, 8 H), 4.11 (q, J = 7.2 Hz, 8 H), 1.20 (t, J = 7.2 Hz, 12 H).

View Article Online

Published on 08 February 2012. Downloaded by State University of New York at Stony Brook on 30/10/2014 15:40:16.

Table 1 Photophysical data for **TPCd** and **TPCd**–Cd^{2+}

Compound	λ_{abs}[a]/nm	$\lambda_{OP\text{-}ex}$[b]/nm	λ_{em}[c]/nm	$\lambda_{TP\text{-}ex}$[d]/nm	Φ[e]	δ[f]/GM
TPCd	365	370	502	740	0.035	102
TPCd–Cd^{2+}	365	370	502	740	0.453	242

[a] Maximum absorption wavelength. [b] Maximum one-photon excitation wavelength. [c] Maximum fluorescence emission wavelength. [d] Maximum two-photon excitation wavelength. [e] Quantum yield. [f] Two-photon absorption cross-section. These data were measured in Tris-HCl (0.02 M) solution (containing 0.1 mM sodium phosphate, pH = 7.4).

4-Nitro-*N*,*N*,*N*′,*N*′-tetra{(2-hydroxyethyl)carbamoylmethyl}-1,2-phenylenediamine (VII)

To a solution of **VI** (2 g, 4.4 mmol) in AcOH (15 mL) was added fuming HNO_3 (0.3 mL, 5 mmol) dissolved in AcOH (2.5 mL) in a dropwise manner at 0 °C over 5–10 min. The reaction was monitored by the disappearance of the starting material on a silica TLC plate. After completion, the reaction mixture was poured on to ice-water. After extraction with CH_2Cl_2, the organic layer was dried over anhydrous Na_2SO_4 and filtered. After removing the solvent under reduced pressure, the residue was purified by column chromatography using petroleum ether–EtOAc 4 : 1 (v/v) as eluant. Yield 1.8 g (82%) of **VII** as yellow crystals. ^{1}H NMR (300 MHz $CDCl_3$): δ 7.96 (s, 1H), 7.84 (d, J = 9 Hz 1H), 7.04 (d, J = 9 Hz 1H), 4.42 (s, 4H), 4.28 (s, 4H), 4.13 (q, J = 7.2 Hz, 8 H), 1.22 (t, J = 7.2 Hz, 12 H).

4-Amino-*N*,*N*,*N*′,*N*′-tetra{(2-hydroxyethyl) carbamoylmethyl}-1,2-phenylenediamine (VIII)

4-Nitro-*N*,*N*,*N*′,*N*′-tetra{(2-hydroxyethyl)carbamoylmethyl}-1,2-phenylenediamine **VII** (420 mg, 0.85 mmol) was dissolved in 20 mL of EtOH. 5% Pd/C (200 mg) was added to the solution and the mixture was stirred overnight under a hydrogen atmosphere. The reaction mixture was filtered and dried over anhydrous Na_2SO_4, purified by column chromatography using petroleum ether–EtOAc 3 : 1 (v/v) as eluant. Yield 308 mg (78%) of **VIII** as brown solid. ^{1}H NMR (300 MHz $CDCl_3$): δ 6.80 (d, J = 8 Hz 1H), 6.29 (s, 1H), 6.18 (d, J = 8 Hz 1H), 4.22 (s, 4H), 4.09 (s, 4H), 4.02 (q, J = 7.2 Hz, 8H), 3.18 (s, 2H), 1.10 (t, J = 7.2 Hz, 12 H). MS (ESI+) Calcd for $C_{22}H_{33}N_3O_8$ ($[M + H]^+$, 468.2; Found: 468.2.

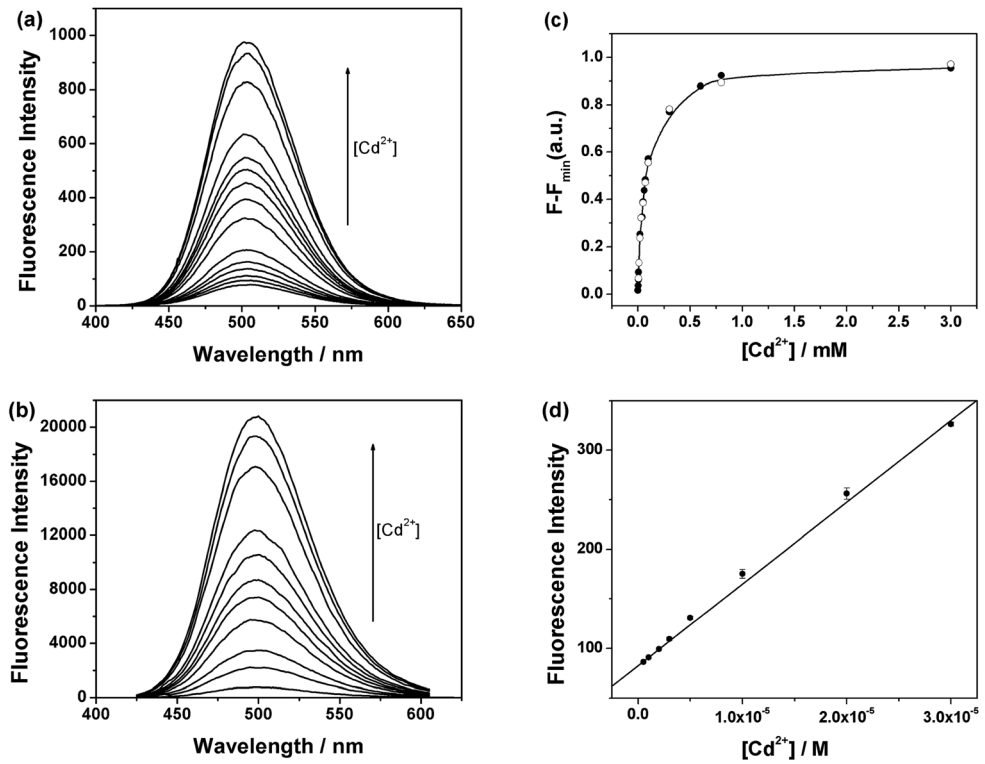

Fig. 3 (a) One-photon fluorescence titration of **TPCd** (10 μM) with free Cd^{2+} (0–0.8 mM) under 370 nm excitation. (b) Two-photon fluorescence titration of **TPCd** with free Cd^{2+} (0–0.8 mM) under 740 nm excitation. (c) Saturation curves for the complexation between **TPCd** (10 μM) and Cd^{2+} under one-photon excitation (●) and two-photon excitation (○). (d) Fluorescence intensity of **TPCd** (10 μM) at 502 nm as a function of Cd^{2+} concentration (0.1–30 μM), data were presented as average ± sd from three independent measurements. These data were measured in Tris-HCl (0.02 M) solution (containing 0.1 mM sodium phosphate, pH = 7.4).

 This journal is © The Royal Society of Chemistry 2012

View Article Online

Published on 08 February 2012. Downloaded by State University of New York at Stony Brook on 30/10/2014 15:40:16.

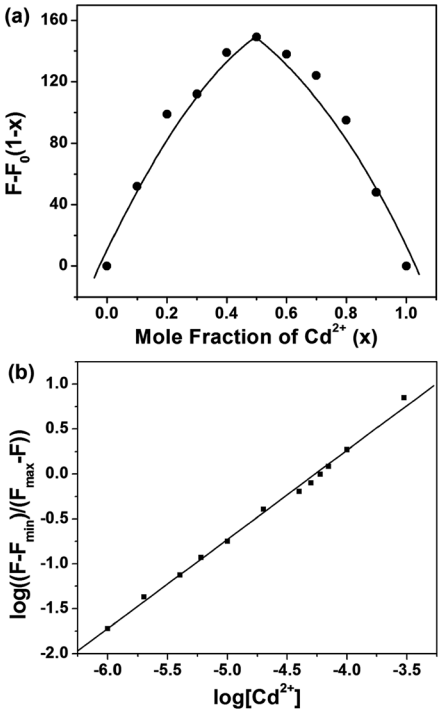

Fig. 4 (a) Job's plot of probe **TPCd** in Tris-HCl (0.02 M) solution (containing 0.1 mM sodium phosphate, pH = 7.4). The total concentration of probe and Cd^{2+} ion was fixed at 10 μM. (b) The Hill plot of probe **TPCd** with free Cd^{2+} in Tris-HCl (0.02 M) solution (containing 0.1 mM sodium phosphate, pH = 7.4) under one-photon excitation at 370 nm.

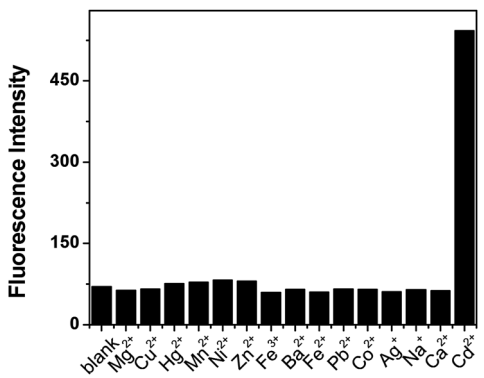

Fig. 5 Fluorescence intensity of **TPCd** (10 μM) in the presence of various metal ions (100 μM) in Tris-HCl (0.02 M) solution (containing 0.1 mM sodium phosphate, pH = 7.4).

TPCd-ester (IX)

A mixture of **IV** (200 mg, 0.78 mmol) and 1-ethyl-3-(3-dimethylaminopropyl)carbodiimide·HCl (265 mg, 1.4 mmol) in DMF (8 mL) was stirred for 30 min. To this mixture, **VIII** (331 mg, 0.67 mmol) and 4-dimethylaminopyridine (10 mg, 0.1 mmol) were added and stirred for 24 h under N_2. The product was extracted with ethyl acetate, the organic layer was dried over anhydrous Na_2SO_4 and filtered, and the solvent was removed in vacuum. The product was purified by column chromatography using chloroform/ethyl acetate (2 : 1) as the eluant. Yield 0.5 g

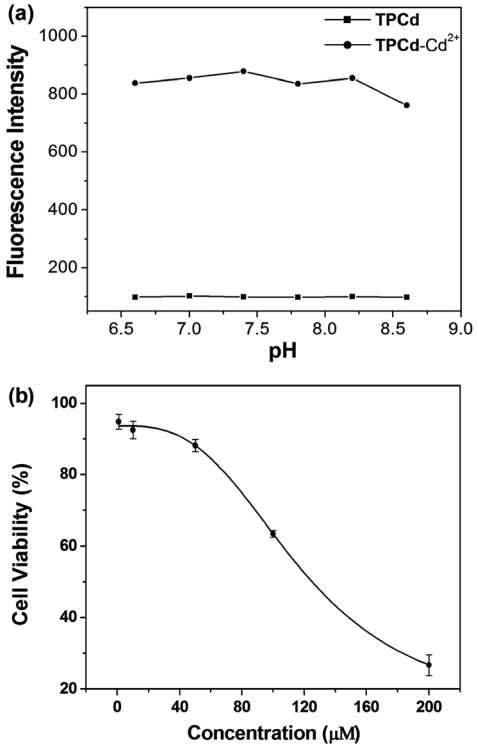

Fig. 6 (a) The effect of pH (6.6–8.6) on the fluorescence intensity of 10 μM **TPCd** and the **TPCd**–Cd^{2+}complex. (b) Cell viability of HepG2 cells cultured with varying concentrations of **TPCd** for 24 h.

(97%) of **IX** as brown oil. ^{1}H NMR (300 MHz $CDCl_3$): δ 8.33 (s, 1H), 8.09 (s, 1H), 7.96 (t, J = 8.7 Hz 1H), 7.83 (d, J = 9 Hz 1H), 7.67 (d, J = 8.7 Hz 1H), 7.18 (s, 1H), 7.11 (t, J = 8.7 Hz 1H), 7.03 (d, J = 8.7 Hz, 1 H), 6.95 (d, J = 9 Hz 1H), 4.26 (s, 6H), 4.20 (s, 4H), 4.04 (q, J = 6.9 Hz, 8 H), 3.20 (s, 3H), 2.65 (s, 3H), 1.14 (t, J = 6.9 Hz 12H). MS (ESI+) Calcd for $C_{37}H_{46}N_4O_{10}$ ([M + Na])$^+$, 729.3; Found: 729.3.

TPCd

300 mg of **IX** (0.71 mmol) was dissolved in 10 mL acetonitrile, and 12 mL 2-aminoethanol was added. The solution was refluxed under nitrogen for 5 h, cooled and concentrated under vacuum to remove the acetonitrile, then poured into 50 mL saturated brine. The mixture was neutralized with TFA, and then concentrated under vacuum. The mixture was purified by column chromatography using methanol/triethylamine/dichloromethane (20 : 3 : 100, v/v/v) as eluant. Yield 98 mg (30%) of **TPCd** as a green solid. ^{1}H NMR (CD_3OD): δ 8.43 (s, 1H), 7.90 (d, J = 9 Hz 2H), 7.67 (d, J = 8.4 Hz 1H), 7.36 (s, 1H), 7.22 (d, J = 8.7 Hz 1H), 7.07 (d, J = 8.4 Hz 1H), 7.02 (s, 1H), 6.94 (d, J = 8.7 Hz, 1 H), 4.27 (s, 2H), 4.08 (s, 4H), 4.04 (s, 4H), 3.45 (q, J = 4.8 Hz, 8 H), 3.25 (s, 3H), 3.20 (t, J = 4.8 Hz, 8H), 2.67 (s, 3H). HRMS (ESI+) Calcd for $C_{37}H_{50}N_8O_{10}$ ([M + Na])$^+$, 789.3545; Found: 789.3542.

Spectroscopic measurements

UV-vis absorption spectra were measured using a TU-1900 UV-vis Spectrophotometer (Beijing Purkinje General Instrument).

View Article Online

Published on 08 February 2012. Downloaded by State University of New York at Stony Brook on 30/10/2014 15:40:16.

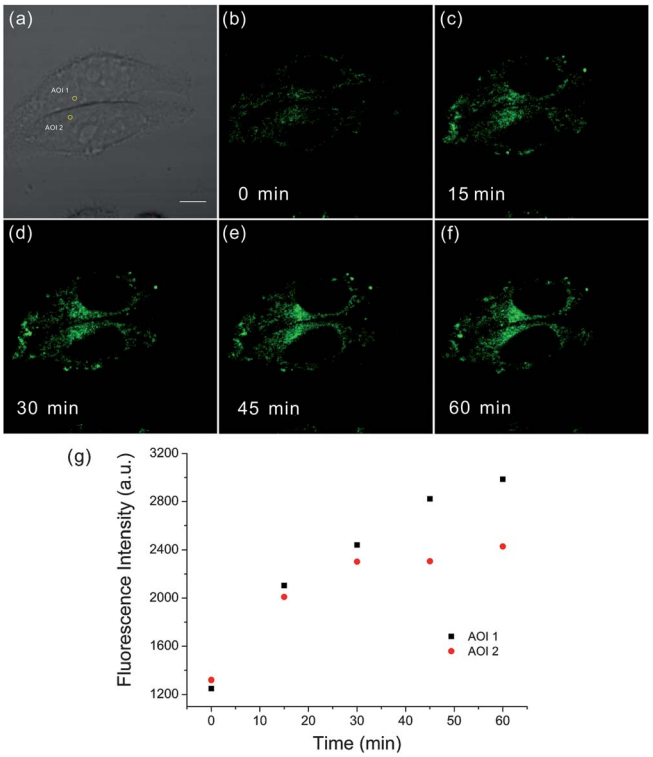

Fig. 7 Confocal fluorescence images of Cd^{2+} in HepG2 cells: (a) bright field; (b) fluorescent images of HepG2 cells loaded with 10 μM **TPCd**; (c–f) fluorescent images of HepG2 cells with further treatment with 50 μM $Cd(NO_3)_2$ solution for 15 min, 30 min, 45 min and 60 min, respectively, under two-photon microscopy; (g) relative TPE fluorescence intensity of **TPCd** in AOI1 and AOI2 regions incubated with Cd^{2+} as a function of time. Excitation wavelength = 740 nm, scale bar, 10 μm.

One-photon excited fluorescence was recorded using a Perkin-Elmer LS 55 fluorimeter equipped with 1-cm cell. A PMT was used as the detector. Two-photon excited fluorescence was measured using a mode-locked Ti: sapphire pulsed laser (Chameleon Ultra II, Coherent Inc.) with a pulse width of 140 fs at a repetition rate of 80 MHz. The two-photon excited fluorescence was recorded using a DCS200PC Photon Counting with single-photon sensitivity through an Omni-λ5008 monochromator (Beijing Zolix Instruments Co., Ltd).

Determination of fluorescence quantum yield and two-photon absorption cross-section

The fluorescence quantum yield (Φ) was measured by the relative method as previously reported.[26] Quinine sulfate in 0.1 M sulfuric acid ($\Phi = 0.55$) was used as reference for **TPCd** and **TPCd**–Cd^{2+}. The fluorescence quantum yield was calculated according to the following equation:

$$\Phi_s = \frac{A_r I_s n_s^2}{A_s I_r n_r^2}\Phi_r \quad (A \leq 0.05)$$

where the subscripts 's' and 'r' refer to the sample and the reference molecule respectively. A is the absorbance of molecules that is controlled below 0.05 for both the sample and reference in the same wavelength. I represents the integrated emission area and n is the refractive index of the solvent.

The two-photon absorption (TPA) cross-section was measured using the two-photon induced fluorescence method. **TPCd** was dissolved in Tris-HCl (0.02 M) solution (containing 0.1 mM sodium phosphate, pH = 7.4) at a concentration of 1.0×10^{-5} M. Rhodamine B in CH_3OH (1.0×10^{-5} M) was used as the reference with the reported value of 77 GM (1 GM = 1×10^{-50} cm^4 s·photon^{-1}) at 740 nm. The TPA cross-section was determined using the following equation:[27]

$$\delta_s = \frac{S_s \beta_r \Phi_r C_r}{S_r \beta_s \Phi_s C_s}\delta_r$$

Similar to the measurement of the fluorescence quantum yield, subscripts 's' and 'r' refer to the sample and the reference molecule respectively. S represents the measured two-photon excited fluorescence intensity, Φ is the fluorescence quantum yield, C is the concentration of the solution, and β is the overall fluorescence collection efficiency of the experimental apparatus. The refractive indexes n of the solvents are used here instead of β because all the experiments of both sample and reference were done under the same instrumental conditions.

Determination of complexation ratio and apparent dissociation constant

The stoichiometry of **TPCd**–Cd^{2+} was measured according to Job's method.[28] The fluorescence intensity of **TPCd** with various mole fraction of Cd^{2+} was recorded, while the total concentration of **TPCd** and Cd^{2+} was maintained to be 1.0×10^{-5} M. To determine the apparent dissociation constant (K_d) value of **TPCd**, a series of solutions containing varying amounts of Cd^{2+} were prepared in the presence of 10 μM **TPCd** in Tris-HCl (0.02 M) solution (containing 0.1 mM sodium phosphate, pH = 7.4). The apparent dissociation constant was determined using the following equation:[29]

$$F - F_{min} = [Cd^{2+}](F_{max} - F_{min})/K_d$$

where F is the observed fluorescence, F_{max} is the maximum fluorescence for the **TPCd**–Cd^{2+} complex at a saturation concentration of Cd^{2+}, and F_{min} is the fluorescence for free **TPCd**.

In order to determine the K_d value for the two-photon mode, the TPE fluorescence intensity was recorded in the range of 420–610 nm, excited by a mode-locked titanium-sapphire laser source with the wavelength set at 740 nm and an output power of 1400 mW.

Cell culture

HepG2 cells were grown in culture flasks containing Dulbecco's modified Eagle's medium supplemented with 10% newborn calf serum, 100 U mL^{-1} penicillin and 100 μg mL^{-1} streptomycin at 37 °C in 5% CO_2. Confluent cells were harvested by treatment with 0.25% (w/v) trypsin for 2 min at room temperature and then cultured in 35 mm Petri dishes overnight. Following rinsing with Tyrode's buffer for three times, adherent cells were incubated with **TPCd** working solution at 37 °C for 1 h. After incubation, cells were rinsed with Cd^{2+}-free Tyrode's buffer for three times and ready for experiments.

 This journal is © The Royal Society of Chemistry 2012

View Article Online

Published on 08 February 2012. Downloaded by State University of New York at Stony Brook on 30/10/2014 15:40:16.

Cd^{2+} imaging by two-photon microscopy

TPCd working solution was diluted from a 4 mM stock solution with Tyrode's buffer to a final concentration of 10 μM. 50 μM Cd^{2+} solution was prepared in Cd^{2+}-free Tyrode's buffer (pH = 7.2). An Olympus FV1000 confocal microscope was employed for Cd^{2+} imaging with two-photon excitation (740 nm), and an emission filter (525/45 nm) was used. Fluorescence images (512 × 512 pixels) were recorded at a rate of 8 μs per pixel using a PMT. Cd^{2+} solutions were manually applied to the adherent cells using a micropipette.

Cytotoxicity assay

Cytotoxicity assay was carried out using Cell Counting Kit-8 (CCK-8, Dojindo, Japan). HepG2 cells (5×10^4 cells mL^{-1}) were seeded onto a 96-well cell culture plate; 3 h later, **TPCd** with concentrations of 1, 10, 50, 100 and 200 μM were added to each well that contained ~5×10^3 cells. After cell culture for 24 h, 10 μL of CCK-8 solution was added to each well, followed by incubation for 2 h. Subsequently the absorbance at 450 nm was measured using an ELISA reader. The reference wavelength was 630 nm. Cell viability (Cv) was calculated according to the equation below:

$$\text{Cv}\ (100\%) = [(A_s - A_b)/(A_c - A_b)] \times 100\%$$

where A_s corresponds to the experimental well containing the cells, CCK-8 and **TPCd**; A_c corresponds to the control well containing the cell, CCK-8; A_b corresponds to the blank well containing CCK-8. All the wells contained culture medium additionally. This experiment was repeated five times.

Results and discussion

Cd^{2+} sensing principle and photophysical properties of TPCd

Several sensing mechanisms have been utilized to construct fluorescent probes, which include internal charge transfer (ICT), photoinduced electron transfer, resonance energy transfer (RET) and so on.[30] In our case, the PET principle is adopted in molecule design, not only because of the simple synthesis by combining the fluorophore and the chelator though a σ bond, but also for its 'off–on' luminescence pattern which is useful for *in vivo* applications. Following this principle, the probe was designed and made up of two sections, an emitting motif and a target recognition domain, with the HOMO (highest occupied molecular orbital) energy level of the two parts matching properly. Before the combination with metal ions, the fluorescence emission of the emitting motif is quenched by the recognition domain through the PET process, therefore the probe itself is weakly fluorescent. Upon binding with target ions, which lowers the HOMO energy of the recognizing domain and thus inhibits the PET process, the fluorescence intensity of the emitter is enhanced such that a turn-on response to target ions occurs (Scheme 2).

As illustrated by the geometries and frontier orbitals (Fig. 1a b) which were calculated at the b3lyp/6-31g (d) level,[31] the HOMO of **TPCd** is equally distributed on the fluorophore and the chelator, and the LUMO (lowest unoccupied molecular orbital) is located on the fluorophore. Upon the excitation of the free probe, electrons transfer from the chelator to the excited fluorophore, impeding the radiative relaxation and thus resulting in fluorescence quenching. After binding to Cd^{2+}, as seen, both HOMO and LUMO are located on the fluorophore, so that the PET process is blocked and the emission of the fluorophore is restored (Fig. 1c,d). In addition to the sensing mechanism, the water-solubility of the molecule is another important concern for a probe designed for intracellular use. The *o*-phenylenediamine derivative is adopted as the Cd^{2+} chelator which offers good water-solubility owing to the abundant hydroxyl groups.[6] As is established, the photophysical properties of the emitting motif, mainly including TP cross-section and quantum yield, are undoubtedly the most important and crucial characters of TPE molecules which decide the sensitivity of detection.[32] In consideration of two-photon photophysical properties, the prodan derivative is employed as the fluorophore of **TPCd** because of its competitive TP cross-section.

The photophysical features of the probe **TPCd** were investigated. The molecule exhibited a linear absorption band with the maximum locating at 365 nm (Fig. 2a). The absorption wavelength of the probe remained almost unchanged after binding with various amounts of Cd^{2+}, which is a typical character of a photo-induced electron transfer process. Since no linear absorption occurred at any wavelength longer than 500 nm (data not shown), the NIR light-excited fluorescence (*vide infra*), with the emission peak locating at 502 nm in aqueous buffer solution (Table 1), can be ascribed to non-linear luminescence. We then examined the Cd^{2+}-induced off–on switch of the probe fluorescence under one-photon excitation at 370 nm. Due to the photo-induced electron transfer from the chelator to the emitter, the fluorescence of the fluorophore was rather weak and the quantum yield was determined as 0.035. After binding to Cd^{2+} which blocked the PET process, the fluorescence intensity of the probe was enhanced by up to 15-fold and the largest quantum yield was obtained as 0.453 (Table 1). Interestingly, the two-photon fluorescence intensity of **TPCd** was enhanced by 27-fold upon Cd^{2+} binding, which is especially valuable for its two-photon application and can be explained with two-photon absorption cross-section (δ) of the fluorophore. As is recognized, the two-photon fluorescence efficiency is related not only to the quantum yield but also to the two-photon absorption cross-section of a molecule. The δ values of **TPCd** before and after combining with Cd^{2+} were determined and list in Table 1, which showed an approximately 2-fold enlargement caused by Cd^{2+} binding. Generally, the TP action cross-section ($\Phi\delta$), which is the product of TP absorption cross-section (δ) and quantum yield (Φ), is regarded as the determinant factor deciding the TPE fluorescence of molecules. Since the quantum yield is considered as identical for one-photon and multi-photon excitation, the 2-fold enlargement of the TP absorption cross-section could be responsible for the magnified two-photon fluorescence enhancement as compared to one-photon fluorescence (27-fold *versus* 15-fold). The action cross-section values of **TPCd** and **TPCd**–Cd^{2+} complex were measured at different wavelengths (Fig. 2b). The maximum action cross-section was obtained at 740 nm, which is twice the maximum linear absorption wavelength and can be taken as an evidence of the two-photon excitation process. As is listed in Table 1, the action cross-section at 740 nm was increased from 3.6 to 109 GM upon Cd^{2+} binding

View Article Online

Published on 08 February 2012. Downloaded by State University of New York at Stony Brook on 30/10/2014 15:40:16.

(1 GM = 1 × 10^{-50} cm^4 s·photon^{-1}), indicating promising prospect of the probe in two-photon applications.

Fluorescence titration of the probe and quantitative Cd^{2+} determination

The fluorescence titration of the probe with free Cd^{2+} was performed with both one-photon and two-photon excitation modes. Under the two excitation modes, the fluorescence enhancement occurred in the same Cd^{2+} concentration-dependent manner (Fig. 3a,b), except that the enhancing multiple of fluorescence intensity under TPE is approximately twice as much as that under OPE, which is consistent with the aforementioned photophysical data. A saturation of binding was achieved at a relatively high Cd^{2+} concentration (Fig. 3c). With the probe being fixed at 10 μM, the plateau in the saturation curves started from 0.8 mM of Cd^{2+} for both OPE and TPE titration, suggesting that the target binding ability of the probe was not affected by the excitation mode. A linear relationship between the enhancement of fluorescence intensity and the concentration of Cd^{2+} can be found within a quite wide range (0.1–30 μM, correlation coefficient = 0.996, Fig. 3d). The relative standard deviations from three repeated measurements were less than 3%, indicating the high reproducibility of the detection. The limit of detection was 0.04 μM calculated according to the $3s_b/m$ criterion, where m is the slope for the range of the linearity used and s_b the standard deviation of blank (n = 11). Such analytical performances are comparable to or better than all the reported fluorescent probes for Cd^{2+}, which provide the possibility to quantitatively detect Cd^{2+} with this probe.

Binding thermodynamics of TPCd with Cd^{2+}

Some physical chemistry parameters of the combination between **TPCd** and Cd^{2+} were also acquired. A Job's plot was used to determine the binding stoichiometry of **TPCd** with Cd^{2+} ions. The total concentration of the probe and Cd^{2+} was held constant while altering the mole fraction of Cd^{2+} ions, and the fluorescence enhancement value was plotted against the mole fraction (Fig. 4a). The maximum fluorescence enhancement was acquired at a Cd^{2+} mole fraction of 0.5, indicating that **TPCd** chelated Cd^{2+} with 1 : 1 stoichiometry. Under one-photon excitation, the dissociation constant K_d was determined using the Hill plot (Fig. 4b). The plot of $\log((F - F_{min})/(F_{max} - F))$ *vs.* $\log[Cd^{2+}]$ exhibited a slope of 1.0, which confirmed a 1 : 1 complexation between **TPCd** and Cd^{2+}. The K_d value was calculated to be 6.1 × 10^{-5} M according to the x axis interception. With the same method, the K_d value for two-photon titration was determined to be 7.2 × 10^{-5} M, quite close to that obtained with one-photon mode.

Selectivity of TPCd toward Cd^{2+}

As chelation-based probes for metal ions, the specificity of the receptor towards the target is of particular importance, because coordination bonds are likely to form between the receptor and other metal ions, especially those with similar radius or orbital configuration. In fact, in quite a few cases of the reported Cd^{2+} fluorescent probes, Zn^{2+} and Hg^{2+} also raised considerable response to the probe duo to their similar orbital distribution and analogous affinity for ligation atom with Cd^{2+}.[8,10] Therefore, to investigate the specificity of **TPCd**, the congeners including Zn^{2+} and Hg^{2+} are considered in the first place. Not surprisingly, when conducting the recognition experiments in pure water, Hg^{2+} caused non-negligible fluorescence enhancement at comparable concentrations, the reason for which may be that Hg^{2+} has a quite similar ionic radius to Cd^{2+} (1.02 Å for Hg^{2+} and 0.96 Å for Cd^{2+}). Nonetheless, Hg^{2+} was easily screened by using Tris-HCl as the buffer solution, which is due to the extremely stable complexation between Hg^{2+} and the $-NH_2$ group in the Tris molecule. It was found that Zn^{2+} did not have a notable response in our case, which could be interpreted as that Zn^{2+} is too small (with an ionic radius of 0.74 Å) to form a tight cage structure with the ligand, *i.e.*, the *o*-phenylenediamine derivative. In subsequent investigations we examined altogether 14 kinds of metal ions, either having a strong coordination ability or possibly coexisting in environmental/biological samples, for their influences. It was found that Pb^{2+} could respond to the probe and thus disturb the detection of Cd^{2+} both in pure water and in Tris-HCl buffer. As is well documented, Pb^{2+} always exhibits the inert pair effect and variable coordination numbers and geometries owing to its electronic configuration and size, and hence it may influence the detection of other metal ions usually smaller than it.[33] A simple yet effective strategy to screen Pb^{2+} is to introduce a certain amount of phosphate, a type of normally used inorganic salt in chemical and biological assays, in the assay buffer,[34] so that Pb^{2+} is thoroughly precipitated due to the very low solubility of $Pb_3(PO_4)_2$ [$K_{sp}(Pb_3(PO_4)_2)$ = 8 × 10^{-43}]. Comprehensively considering the above factors, a mixed buffer (0.02 M Tris-HCl containing 0.1 mM sodium phosphate) was adopted for Cd^{2+} sensing in our work. In this situation, quite good selectivity was acquired for Cd^{2+} (Fig. 5).

Two-photon microscopy imaging for Cd^{2+} uptake in HepG2 cells

The probe molecule may be suitable for intracellular use since it has good solubility in physiological solutions (up to 5 mg mL^{-1} in water). To explore the applicability of the probe in intracellular imaging, we first studied the pH-dependence of the molecule as well as its cytotoxicity. Obviously, a stable signal, *i.e.*, pH-independent fluorescence in the physiological pH range is essential for an *in vivo* probe. As revealed in our experiments, the fluorescence intensities of both the **TPCd** and **TPCd**–Cd^{2+} complex remained stable from pH 6.6 to 8.6 (Fig. 6a), excluding the possible pH-induced fluorescence alterations in practical use. The cytotoxicity of **TPCd** was investigated by CCK-8 assay. It was observed that the cell viability remained at 90% after 24 h culture even at a **TPCd** concentration as high as 50 μM (Fig. 6b), which is much higher than the normally used probe concentration in cell imaging (10 μM was used in our experiments). It demonstrated that the probe molecule is non-toxic to living cells at reasonable concentration levels. The above results have therefore warranted the application of **TPCd** in living cells.

Intracellular Cd^{2+} imaging experiments were carried out using HepG2 cells as a model. After incubation of HepG2 cells with **TPCd** (10 μM) for 1 h at 37 °C followed by exhaustive washing of the cells, weak green fluorescence can be detected in cells under a confocal microscope excited at 740 nm (Fig. 7b), indicating a successful load of the probe. The cellular uptake of exogenous Cd^{2+} was then observed by introducing 50 μM Cd^{2+} into the cell

 This journal is © The Royal Society of Chemistry 2012

View Article Online

Published on 08 February 2012. Downloaded by State University of New York at Stony Brook on 30/10/2014 15:40:16.

culture. Along with the incubation time from 15–60 min, the green fluorescence became increasingly intensive (Fig. 7c–f), displaying the enhancement of intracellular Cd^{2+} levels. The results also indicated that most cadmium is localized in the area of cytoplasm near the nucleus and, accordingly, the fluorescence intensity at AOI1 and AOI2 regions in this area showed a time-dependent increase (Fig. 7g). Such results are consistent with the reported mechanism of cadmium uptake.[35]

Conclusion

We have made a two-photon excited probe that can function as a fluorescent off–on switch for Cd^{2+} based on a PET mechanism. This probe presented 27-fold TPE fluorescence enhancement in response to Cd^{2+} and possessed favorable quantum yield, two-photon action cross-section and water-solubility. It also showed high selectivity towards Cd^{2+}, good pH-stability within the physiological range and low cytotoxicity. Satisfying analytical performances of Cd^{2+} determination were acquired, including a wide linear range, high sensitivity and good reproducibility. The probe was successfully applied in intracellular Cd^{2+} imaging in living HepG2 cells with two-photon microscopy. It could potentially be used in signaling Cd^{2+}-related cellular or environmental events.

Acknowledgements

The authors thank the National Science Foundation of China (No. 21075094), National Basic Research Program of China (2011CB910403) and the Science Fund for Creative Research Groups (No. 20621502 and 20921062) for financial support.

References

1 T. Jin, J. Lu and M. Nordberg, *Neurotoxicology*, 1998, **19**, 529.
2 M. P. Waalkes, *Mutat. Res.*, 2003, **533**, 107; M. Waisberg, P. Joseph, B. Hale and D. Beyersmann, *Toxicology*, 2003, **192**, 95.
3 A. N. Anthemidis and C. P. Karapatouchas, *Microchim. Acta.*, 2008, **160**, 455; G. Kaya and M. Yaman, *Talanta*, 2008, **75**, 1127.
4 A. C. Davis, C. P. Calloway and B. T. Jones, *Talanta*, 2007, **71**, 1144.
5 A. P. de Silva, H. Q. N. Gunaratne, T. Gunnlaugsson, A. J. M. Huxley, C. P. McCoy, J. T. Rademacher and T. E. Rice, *Chem. Rev.*, 1997, **97**, 1515; J. Zhang, R. E. Campbell, A. Y. Ting and R. Y. Tisen, *Nat. Rev. Mol. Cell Biol.*, 2002, **3**, 906; P. Jiang and Z. Guo, *Coord. Chem. Rev.*, 2004, **248**, 205.
6 T. Cheng, Y. Xu, S. Zhang, W. Zhu, X. Qian and L. Duan, *J. Am. Chem. Soc.*, 2008, **130**, 16160.
7 C. Lu, Z. Xu, J. Cui, R. Zhang and X. Qian, *J. Org. Chem.*, 2007, **72**, 3554.
8 M. Taki, M. Desaki, A. Ojida, S. Iyoshi, T. Hirayama, I. Hamachi and Y. Yamamoto, *J. Am. Chem. Soc.*, 2008, **130**, 12564.
9 X. Peng, J. Du, J. Wang, Y. Wu, J. Zhao, S. Sun and T. Xu, *J. Am. Chem. Soc.*, 2007, **129**, 1500.
10 S. Y. Park, J. H. Yoon, C. S. Hong, R. Souane, J. S. Kim, S. E. Matthews and J. Vicens, *J. Org. Chem.*, 2008, **73**, 8212.
11 F. Helmchen and W. Denk, *Nat. Methods*, 2005, **2**, 932.
12 A. R. Clapp, T. Pons, I. L. Medintz, J. B. Delehanty, J. S. Melinger, T. Tiefenbrunn, P. E. Dawson, B. R. Fisher, B. O'Rourke and H. Mattoussi, *Adv. Mater.*, 2007, **19**, 1921.
13 L. Z. Liu, G. H. Wei, Z. H. Liu, Z. K. He, S. Xiao and Q. Q. Wang, *Bioconjugate Chem.*, 2008, **19**, 574; L. Z. Liu, M. Shao, X. H. Dong, X. F. Yu, Z. H. Liu, Z. K. He and Q. Q. Wang, *Anal. Chem.*, 2008, **80**, 7735; L. Z. Liu, X. H. Dong, W. L. Lian, X. N. Peng, Z. H. Liu, Z. K. He and Q. Q. Wang, *Anal. Chem.*, 2010, **82**, 1381; L. Z. Liu, H. Li, T. Qiu, G. H. Zhou and Z. H. Liu, *Chem. Commun.*, 2011, **47**, 2622.
14 T. P. Thomas, M. T. Myaing, J. Y. Ye, K. Candido, A. Kotlyar, J. Beals, P. Cao, B. Keszler, A. K. Patri, T. B. Norris and J. R. Baker, *Biophys. J.*, 2004, **86**, 3959.
15 S. M. Potter, C. M. Wang, P. A. Garrity and S. E. Fraser, *Gene*, 1996, **173**, 25.
16 H. M. Kim, B. R. Kim, J. H. Hong, J. S. Park, K. J. Lee and B. R. Cho, *Angew. Chem., Int. Ed.*, 2007, **46**, 7445.
17 H. M. Kim, C. Jung, B. R. Kim, S. Y. Jung, J. H. Hong, Y. G. Ko, K. J. Lee and B. R. Cho, *Angew. Chem., Int. Ed.*, 2007, **46**, 3460.
18 H. M. Kim, M. S. Seo, M. J. An, J. H. Hong, Y. S. Tian, J. H. Choi, O. Kwon, K. J. Lee and B. R. Cho, *Angew. Chem., Int. Ed.*, 2008, **47**, 5167.
19 C. S. Lim, D. W. Kang, Y. S. Tian, J. H. Han, H. L. Hwang and B. R. Cho, *Chem. Commun.*, 2010, **46**, 2388.
20 M. K. Kim, C. S. Lim, J. T. Hong, J. H. Han, H. Y. Jang, H. M. Kim and B. R. Cho, *Angew. Chem., Int. Ed.*, 2010, **122**, 374.
21 H. J. Kim, J. H. Han, M. K. Kim, C. S. Lim, H. M. Kim and B. R. Cho, *Angew. Chem., Int. Ed.*, 2010, **122**, 6938.
22 C. B. Huang, J. L. Qu, J. Qi, M. Yan and G. X. Xu, *Org. Lett.*, 2011, **13**, 1462.
23 J. F. Zhang, C. S. Lim, S. Bhuniya and B. R. Cho, *Org. Lett.*, 2011, **13**, 1190.
24 K. D. Belfield, M. V. Bondar, A. Frazer, A. R. Morales, O. D. Kachkovsky, I. A. Mikhailov, A. E. Masunov and O. V. Przhonska, *J. Phys. Chem. B*, 2010, **114**, 9313.
25 X. H. Dong, Y. Y. Yang, J. Sun, Z. H. Liu and B. F. Liu, *Chem. Commun.*, 2009, 3883; L. Z. Liu, X. H. Dong, Y. Xiao, W. L. Lian and Z. H. Liu, *Analyst*, 2011, **136**, 2139.
26 J. N. Demas and G. A. Crosby, *J. Phys. Chem.*, 1971, **75**, 991.
27 C. Xu and W. W. Webb, *J. Opt. Soc. Am. B*, 1996, **13**, 481.
28 B. Valeur, *Molecular Fluorescence: Principles and Applications*, Wiley-VCH, Weinheim, 2002.
29 R. Y. Tsien, T. Pozzan and T. J. Rink, *J. Cell Biol.*, 1982, **94**, 325; S. Bagh and M. F. Paige, *J. Phys. Chem. A*, 2006, **110**, 7057.
30 A. P. de Silva, D. B. Fox, A. J. M. Huxley and T. S. Moody, *Coord. Chem. Rev.*, 2000, **205**, 41.
31 M. J. Frisch *et al.*, *Gaussian 09* (Revision A.02). Gaussian, Inc., Wallingford CT, 2009.
32 J. R. Lakowicz, *Principles of Fluorescence Spectroscopy*, Springer-Verlag, Berlin-Heidelberg, 3rd edn, 2006.
33 J. Sanchiz, P. Esparza, D. Villagra, S. Domínguez, A. Mederos, F. Brito, L. Araujo, A. Sánchez and J. M. Arrieta, *Inorg. Chem.*, 2002, **41**, 6048.
34 H. Sigel, C. P. Da Costa and R. B. Martin, *Coord. Chem. Rev.*, 2001, **219–211**, 435.
35 P. F. Dehn, C. M. D. White, E. Conners, G. Shipkey and T. A. Cumbo, *In Vitro Cell. Dev. Biol.: Anim.*, 2004, **40**, 172.